Applied Surface Science 672 (2024) 160740

Contents lists available at ScienceDirect

Applied Surface Science

journal homepage: www.elsevier.com/locate/apsusc

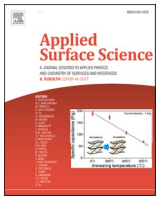

Full Length Article

Why the adhesion strength is not enough to assess ice adhesion on surfaces

Luca Stendardo [a,b], Giulia Gastaldo [b], Marc Budinger [c], Irene Tagliaro [a], Valérie Pommier-Budinger [b,*], Carlo Antonini [a,*]

[a] Department of Materials Science, University of Milano - Bicocca, via R. Cozzi 55, 20125 Milano, Italy
[b] Fédération ENAC ISAE-SUPAERO ONERA, Université de Toulouse, 10 AvenueEdouard Belin, 31400 Toulouse, France
[c] ICA, Université de Toulouse, UPS, INSA, ISAE-SUPAERO, MINES-ALBI, CNRS, 3 rue Caroline Aigle, 31400 Toulouse, France

ARTICLE INFO

Keywords:
Ice adhesion
Icephobicity
Icing
Coatings
Ice fracture

ABSTRACT

The interest in the development of icephobic surfaces has pushed towards the definition of standardized processes and parameters to assess ice adhesion, with the ambition of identifying an equivalent method to contact angle measurements used to assess wetting properties. Although most studies focus on the average ice adhesion strength, measured as the force per unit area required to detach ice, much less attention is paid to interfacial toughness, perhaps as its measurement is challenging. In this article, we provide a conceptual framework to correctly measure both ice adhesion strength and interfacial toughness, even using a simple push test method, laying the ground for a complete and comprehensive assessment of surface icephobicity.

1. Introduction

Ice can have negative effects that endanger both equipment and human life. In the last decade, icephobic materials and coatings have experienced a broad interest in the research community, resulting in many different test methods to characterize and evaluate novel surfaces [1–3]. Recent reviews have shown that different test systems can produce ice adhesion values that vary by as much as an order of magnitude for the same substrate [1,4].

These discrepancies are generally attributed to the influence of stress concentrations [5], often without specifying their magnitude or even the qualitative properties of the stress distribution [1,6]. In a previous study we analyzed the stress distributions at the ice-substrate interface for a cylindrical ice sample on a horizontal shear test (representation of the configuration in Fig. 1A) using a hybrid numerical and experimental approach [7]. The stress distribution was mapped for different pushing heights (distance between the force application point and the substrate) and we found that in the tested conditions the minimum shear stress, rather than the average or the maximum shear stress at the interface, controls ice adhesion. As a results, ice detachment occurs when the critical stress is exceeded over the entire interface. Depending on the geometry of the ice block, however, we also observed that critical stress is no longer the determining quantity when propagation of the crack is visible [7].

It is important to understand the fundamental fracture mechanics that control the detachment of ice when performing ice adhesion tests. In general, two different fracture mechanisms can be identified: stress- or toughness-dominated fracture [7–16]. The interface characteristic length scale plays a primary role [9]. Small interfaces typically exhibit a stress-dominated behavior, where the failure of the interface is instantaneous. Differently, larger interfaces are controlled by toughness and are characterized by a gradual crack propagation (Fig. 1B and 1C) [9,17–19]. To determine whether the fracture is controlled by stress or toughness, the concept of cohesive length can be employed [9,12,17]. According to this theory, the critical length L_c, at which the transition between the two fracture regimes occurs, scales as

$L_c \propto G_c E_{ice} h/\tau^2$, where G_c is the interfacial toughness, E_{ice} is the elastic modulus of the ice, h is the height of the ice block, and τ is the adhesion strength.

Measuring and comparing shear adhesion strength is only meaningful under stress-dominated conditions. Otherwise, in the case of toughness-dominated fractures, the detachment of the ice is controlled by the strain energy release during crack formation [8,10,11,14]. Nonetheless, most studies do not report any consideration relative to the detachment conditions.

Literature suggests that even when ice adhesion tests are repeated multiple times in the exact same manner, the standard deviation can be up to ±20 % depending on the ice type [1,4]. Several factors, e.g., the water flow before freezing, micro-scale surface roughness, heat transfer processes, and/or the ice crystal structure have been identified as a

* Corresponding authors.
E-mail addresses: valerie.budinger@isae-supaero.fr (V. Pommier-Budinger), carlo.antonini@unimib.it (C. Antonini).

https://doi.org/10.1016/j.apsusc.2024.160740
Received 30 May 2024; Received in revised form 2 July 2024; Accepted 14 July 2024
Available online 24 July 2024

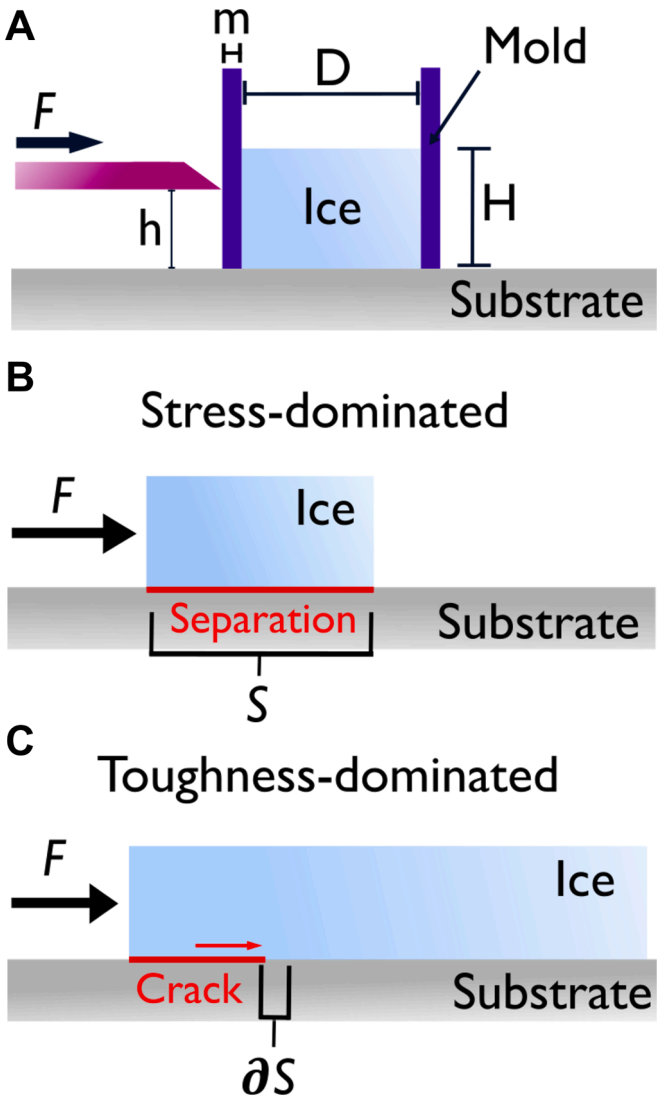

Fig. 1. (A) Representation of a model horizontal push test with cylindrical bulk ice sample. D is the inner diameter of the mold, h denotes the force probe pushing height, m is the mold thickness, and the height of the ice column inside the mold is denoted by H. (B) For small interfaces, the fracture is typically stress-dominated. In these conditions, instantaneous separation of the ice from the substrate occurs, without crack propagation. (C) Large interfaces fail by toughness-dominated fracture. This mechanism is characterized by a gradual propagation of the crack.

possible cause of this large standard deviation [4,20,21]. A recently published round-robin ice adhesion study with identical test surfaces and different test configurations confirms that assessing ice adhesion simply as the average shear stress $\tau = F/A$ results in discrepancies up to an order of magnitude [22]. This result confirms once again that the average shear strength is not a material intrinsic property.

To have a complete characterization of the substrate, the ideal ice adhesion measurement setup should allow to characterize both the critical adhesion stress as well as the toughness. In this study, we lay the ground for a more comprehensive assessment of surface icephobicity, aiming to define a standardization of icephobicity measurement for the icing community. The first contribution of this work is the precise measurement of the adhesion strength by analyzing the stress distribution at the ice-substrate interface and mapping the stress concentration factors for different test geometries. The second contribution concerns the toughness measurements carried out by changing the geometry of the ice block and measuring the force necessary to propagate the interface crack. This novel conceptual framework is generally valid for mechanical push tests, and has been here specifically applied to the commonly used horizontal shear test with cylindrical ice columns [1,4].

2. Experimental and numerical methods

A custom-built horizontal push test has been used for this study to verify the fracture mechanisms and validate the numerical model. The same experimental setup has been already described elsewhere [7,23,34].

During ice accretion and testing, relative humidity was kept below 3 % relative to ambient temperature $T_{amb} = 20°C$. The substrate temperature T_{sub} was set at −10 °C and a freezing time of at least 20 min was chosen to ensure complete freezing of the water column. Cylindrical nylon (PA.6) molds (inner diameters D = 8–14 mm, wall thickness m = 2 mm) were used to form the ice columns. Water was poured inside the nylon molds at about 0 °C and then cooled down to T_{sub}. The nylon molds remained in place during the ice adhesion measurements and their minor influence on the results was analyzed in the Supplementary Material (SM) Sections S1, and S4. The actuation speed of the force probe was set to 5 μm/s. The detachment mechanism was identified using a high-speed camera (PHOTRON NOVA FASTCAM S6, Venus Laowa 100 mm f/2.8 2X Ultra Macro APO lens).

A numerical Finite Element Model (FEM) similar to that of Stendardo et al. [7] was used to calculate the Shear Stress Intensity Factors (SSIFs) and the Toughness Parameters (TP) (see SM Sections S1, S2, and S3 for details).

3. Results and discussion

The test protocol includes two measurements with the same horizontal push test: i) stress-dominated ice detachment induced by a small ice sample (diameter D = 6 – 10 mm); ii) toughness-dominated ice detachment, with a big ice block ($D > 10$ mm). For both cases, the force necessary to remove the ice is recorded. For the stress-dominated case, the critical shear stress is calculated with the Shear Stress Intensity Factors (SSIFs). Similarly, the interfacial toughness is calculated with the help of the Toughness Parameters (TP).

The SSIFs as well as the toughness parameters are a function of the geometry of the test system, i.e., the ice sample height H and diameter D and the pushing height h. The proposed methodology can be applied to already existing push tests or can assist the design of new set-ups, improving the evaluation of icephobic properties of materials and coatings.

3.1. Stress-dominated fracture

In a stress-dominated regime, the entire interface fractures instantaneously, without crack propagation (Fig. 1B) [7,9,11]. A necessary condition in this case is that at every point x of the interface S the stress value exceeds the critical value that leads to failure [7,8]:

$$\boldsymbol{\tau} > \boldsymbol{\tau_c}, \ \forall \ \boldsymbol{x} \in \boldsymbol{S} \tag{1}$$

To characterize a surface for its ice adhesion strength, it is therefore important to find the minimum shear stress τ_{min} over the entire interface while performing the ice adhesion tests. According to Eq. (1), this τ_{min} corresponds to the critical shear stress τ_c characterizing the interface.

The common ice adhesion tests, such as the horizontal push test, allow to record the maximum removal force F_{max}, which is typically used to calculate the average shear strength across the entire interface $\tau_{ave} = F_{max}/A$, where A is the ice-substrate contact area. This average shear stress τ_{ave}, however, is not a pure surface property but depends on geometric parameters, such as pushing height, ice block diameter and height (Fig. 1A).

Dimensionless Shear Stress Intensity Factors (SSIFs) for the hori-

zontal push test are proposed in this study to calculate τ_{min} from τ_{ave}, making the adhesion strength measurements dependent only from the aspect ratios of the geometric parameters and limiting the number of parameters involved in the measurement. The SSIF is defined as τ_{ave}/τ_{min} and is a function of h/D and H/D (Fig. 1A). Applying the Buckingham Π-Theorem (see SM Section S1) leads to [24–26]:

$$\boldsymbol{SSIF} = \frac{\boldsymbol{\tau_{ave}}}{\boldsymbol{\tau_{min}}} = \boldsymbol{f}\left(\frac{\boldsymbol{h}}{\boldsymbol{D}}, \frac{\boldsymbol{H}}{\boldsymbol{D}}\right) \tag{2}$$

A numerical FEM model (see details in SM Section S2 and refer to [27–29]), similar to Stendardo et al. [7], is used to calculate the SSIF for different combinations of h/D and H/D. The main results are presented in Fig. 2B.

The dimensional analysis shows how the SSIF is independent of the load applied to the ice block and how the function $f\left(\frac{h}{D}, \frac{H}{D}\right)$ can be applied to various ice block diameters. A more careful evaluation of the Fig. 2B reveals how for an ice filling height $H/D > 0.5$, the SSIF mainly depends on the pushing height h/D. While doing experiments with the horizontal push test, the SSIF is determined only by the pushing height h/D, as long as $H/D > 0.5$. The minimum shear stress is then calculated as:

$$\boldsymbol{\tau_{min}} = \frac{\boldsymbol{\tau_{ave}}}{\boldsymbol{SSIF}} \tag{3}$$

In this work, only cylindrical ice samples have been analyzed. However, the model can be adapted to any ice sample shape. It is valid for bulk (or glaze) ice (elastic modulus $E_{ice} > 4.5GPa$), and for all surfaces with elastic modulus $E_{sub} > 35GPa$, such as composite materials or metals (see SM Section S4). A validation of the dimensional analysis is available in SM Section S5.

The SSIF map shown in Fig. 2B is validated by a series of ice adhesion experiments carried out on a sample of Al-6060 aluminum alloy. Each measurement is conducted in a stress-dominated fracture regime and at varying geometrical parameters of the test system, i.e., the diameter D, the pushing height h/D, and the ice column height H/D. In each case, a comparable minimum shear stress value, τ_{min}, should be calculated by the model, as this value is exclusively dependent on the substrate and not on the test system geometry.

Table 1 summarizes the results obtained from five ice adhesion tests conducted on the same substrate (Al-6060), with variations in the geometrical parameters. It is evident that the applied force and the measured average shear stress, τ_{ave}, vary considerably between individual measurements, with a standard deviation of ±38.7 % and ±13.6 %, respectively. This confirms that the test system configuration plays a significant role in influencing these values. However, the model is capable of accounting for these geometrical differences and calculating a nearly constant value of the minimum shear stress, τ_{min}, with a standard deviation of only ±7.5 %.

3.2. Toughness-dominated fracture

A force applied on an ice block that is frozen on a substrate induces a static elastic deformation of the ice block, characterized in this case by a potential energy W_P. According to the energy criterion proposed by Griffith [11,29], the formation of a crack along the interface ∂S implies a change in potential elastic energy ∂W_p. The condition for crack formation can therefore be summarized as:

$$-\frac{\partial \boldsymbol{W_P}}{\partial \boldsymbol{S}} = \boldsymbol{G} \geq \boldsymbol{G_c} \tag{4}$$

where G_c is the critical fracture energy per unit surface, also called

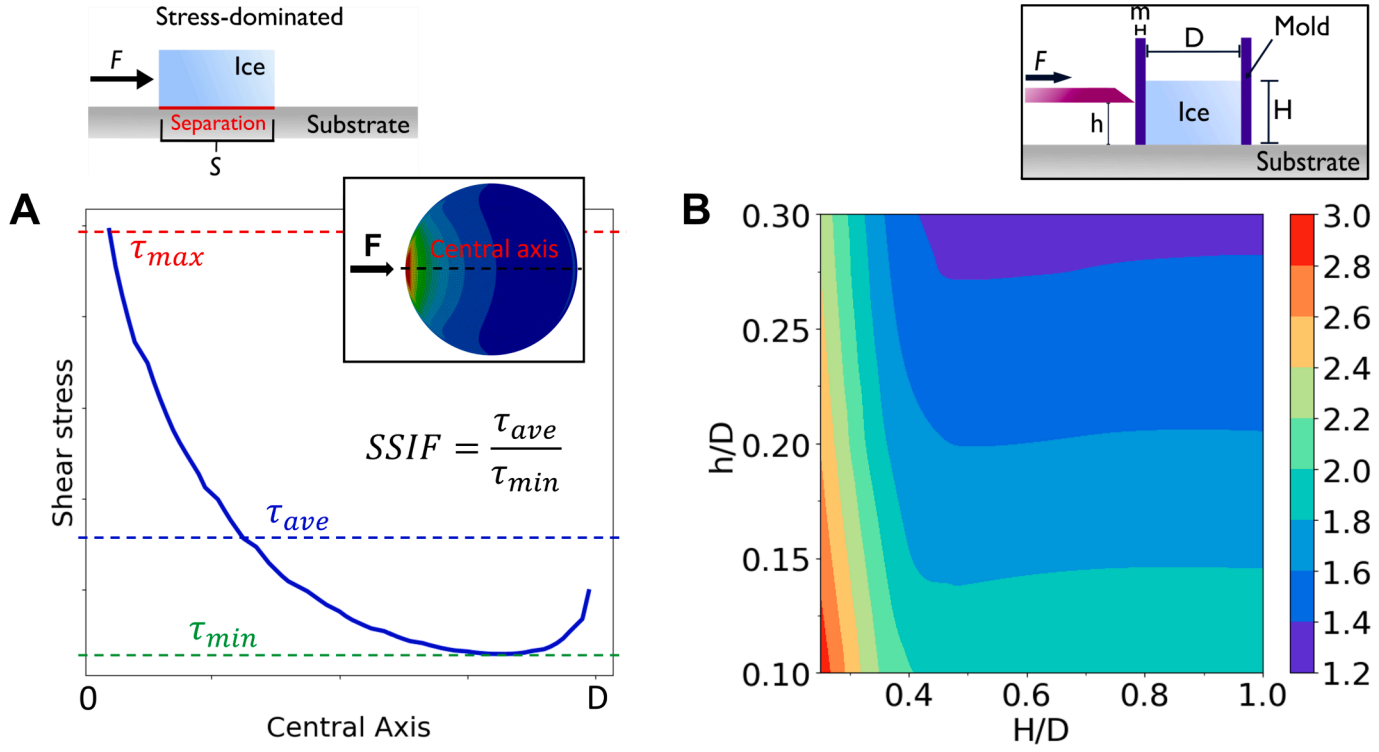

Fig. 2. (A) Definition of the dimensionless SSIF which corresponds to the ratio of average shear stress to minimum shear stress. In this example, the shear stress distribution at the ice-substrate interface of a cylindrical ice sample is visualized along the central axis. Typically, strong stress concentrations are close to the force application point. The shear strength value calculated as $\boldsymbol{\tau} = \boldsymbol{F}/\boldsymbol{A}$ corresponds to the average shear stress $\boldsymbol{\tau_{ave}}$ over the whole interface [7]. In stress-dominated fracture, $\boldsymbol{\tau_{min}}$ controls the detachment. Inset: Example of a numerically calculated shear stress distribution in a cylindrical sample at the ice-substrate interface. (B) The SSIF map is given as a function of h/D and H/D (see SM Section S3 for plotting method). Inset: Representation of a horizontal push test with a cylindrical bulk ice sample.

Table 1
Experimental data and computed τ_{min}. For each test system configuration characterized by a *SSIF*, the experimental data are used to measure τ_{ave} and the numerical model is used to calculate the minimum shear stress, τ_{min}, which is only dependent on the substrate and not on the test system geometry. The ratio of the standard deviation to the mean value ($\sigma(x)/\bar{x}$) was calculated for τ_{ave} and τ_{min}.

	Ice Diameter [mm]	h/D	H/D	Applied Force [N]	$SSIF = \tau_{ave}/\tau_{min}$	τ_{ave} [kPa]	τ_{min} [kPa]
	8	0.125	0.525	55.02	1.9	1095	**576**
	8	0.25	0.625	48.56	1.2	966	**644**
	8	0.375	0.625	38.82	1.2	772	**644**
	10	0.1	0.4	91.36	1.9	1163	**581**
	12	0.083	0.46	107.34	1.8	949	**527**
$\sigma(x)/\bar{x}$						13.6 %	**7.5 %**

toughness. For a crack to propagate along the entire interface, the condition $G \geq G_c$ must hold for every change in interface ∂S.

A numerical FEM model to calculate the interfacial toughness is developed and described in SM Section S2. The model allows to retrieve the interfacial toughness starting from the experimentally measured force F necessary to propagate the crack along the entire interface (measured in [N]) under toughness-dominated fracture (hence, when a gradual crack propagation is visible).

In general, three different crack opening modes can be identified (see SM Section S6): normal opening (mode I) and shear opening (mode II and III) [12,14]. The mode III component is an out-of-plane shear component and can be neglected in this study as the loading conditions are such that the force acts along an axis of symmetry of the ice block. In case of the horizontal push test, the relative components of opening modes I and II depend on the pushing height [7], but in general the debonding condition was observed to be always a mixed mode opening [7,9,12,14]. The model presented in this work computes the total change in potential elastic energy, without differentiating between normal (G_I) and shear (G_{II}) opening. Therefore, the energy release rate (toughness) calculated with this method is a global G_T value.

By applying the Buckingham Π-Theorem, the dimensionless function that corresponds to the Toughness Parameter (TP) is derived (see SM Section S1):

$$TP = \frac{G_c D^3}{F^2} E_{ice} = g\left(\frac{h}{D}, \frac{H}{D}, \frac{m}{D}, \frac{E_{ice}}{E_{nylon}}\right) \tag{5}$$

where G_c represents the interfacial toughness, F the force necessary to propagate the crack along the entire interface, h, H, D, m are the geometrical parameters introduced in Fig. 1A, and E_{ice}, E_{nylon} are the elastic moduli of the ice and the nylon mold, respectively.

To plot the contour lines for the toughness dominated case, in a similar way to Fig. 2B, the function needs to be dependent of two variables only. Given that this analysis is carried out only for nylon molds and that the ice formed is always bulk ice, E_{nylon}/E_{ice} can be considered a system constant and, therefore, removed from the equation. In the same way, this study on interfacial toughness is based on three different molds with diameter D of 10, 12, and 14 mm, and constant wall thickness m of 2 mm. This results in three different cases of m/D, respectively 0.2, 0.167, and 0.143. By plotting three different graphs for each case of m/D, Eq. (5) can be further reduced to:

$$TP = \frac{G_c D^3}{F^2} E_{ice} = g\left(\frac{h}{D}, \frac{H}{D}\right) \tag{6}$$

The simplifications from Eqs. (5) to (6) can be done by restricting the analysis of toughness parameters to the specific geometry of interest, e.g. in our case when the cylindrical ice blocks used for testing are formed by using nylon molds and only when the same ratios of m/D are selected. Moreover, similar to the stress-dominated case, this analysis is valid for rigid substrates that have an elastic modulus $E_{sub} > 35GPa$ (see SM Section S4). Nonetheless, the analysis can be easily extended to other geometries, and the results and conclusions presented here remain valid, without losing generality (refer to Section 3.3).

Fig. 3 shows the contour plots of the left-hand side of Eq. (6) as a function of h/D and H/D for different ratios of m/D. The toughness parameters have been calculated numerically by simulating crack propagation with different combinations of h/D, H/D, and m/D.

To experimentally measure the interfacial toughness, the correct toughness parameter is selected from the plots in Fig. 3 based on the experimentally selected values of h/D, H/D, and m/D. During the adhesion tests, the ice removal force F is recorded. The toughness parameter is then equated to the left-hand side Eq. (6), where the measured force F and E_{ice} (typically 9 GPa for bulk ice) is inserted, and thus the corresponding toughness G_c is found. It is worth to notice that for a constant test system geometry and constant ice type, G_c scales with F^2 (see SM Section S1).

In the regions where $h/D > H/D$, the pusher applies the force at a distance from the substrate that is higher than the ice thickness H. This configuration is not recommended for horizontal shear tests [32] and, therefore, the corresponding regions in the plots have been desaturated.

Preliminary experimental tests on aluminum (see SM Section S7) have shown that for a ratio $H/D > 0.25$, it is not possible to have a toughness-dominated fracture propagation. This is in accordance with the literature, stating that the detachment is toughness-dominated for small thicknesses H compared to the length D of the ice block [9,12,33]. To measure the toughness of an interface in an accurate way, it is therefore recommended to choose the experimental parameters such that $H/D < 0.25$. More importantly, this result suggests that a stress- or a toughness-dominated fracture mechanism can be induced simply by modifying the geometry of the ice sample. This is an important consideration in the analysis of the discrepancies between different test systems. If this variable is not considered, the fracture mechanism may be uncontrolled or overseen. Conversely, experimentalists can measure both the adhesion strength and the toughness of the interface with the same test setup by precisely controlling the geometry of the ice sample.

Depending on the substrate, the crack propagation in the toughness dominated regime can be too quick to be visible by eye, and high-speed camera visualization might be necessary to verify the fracture mechanism [7] (see the supporting videos in the SM). Another way to identify the fracture mechanism is to perform adhesion tests with different ice block sizes, as already demonstrated in previous studies [9,12,17]. Going from small to big interface areas, as long as the ice removal force F scales with the contact area of the ice block, the fracture is stress-dominated. On the other hand, if by increasing the interface area the force F does not increase accordingly, the fracture is toughness dominated [9,12,17].

The toughness values on aluminum that can be found in the literature have been obtained with test methods that detach the ice from the substrate in normal direction, therefore toughness values are mainly G_I values. Golovin et al. [9] calculated the total toughness G_T on a variety of surfaces with a horizontal push test; however, aluminum was not among the tested substrates. Table 2 summarizes experimentally obtained toughness values for aluminum substrates and bulk ice found in literature.

The numerical model used in this study is verified by performing a series of experimental measurements of the ice removal force on aluminum (Al-6060) in a toughness-dominated regime. The results of

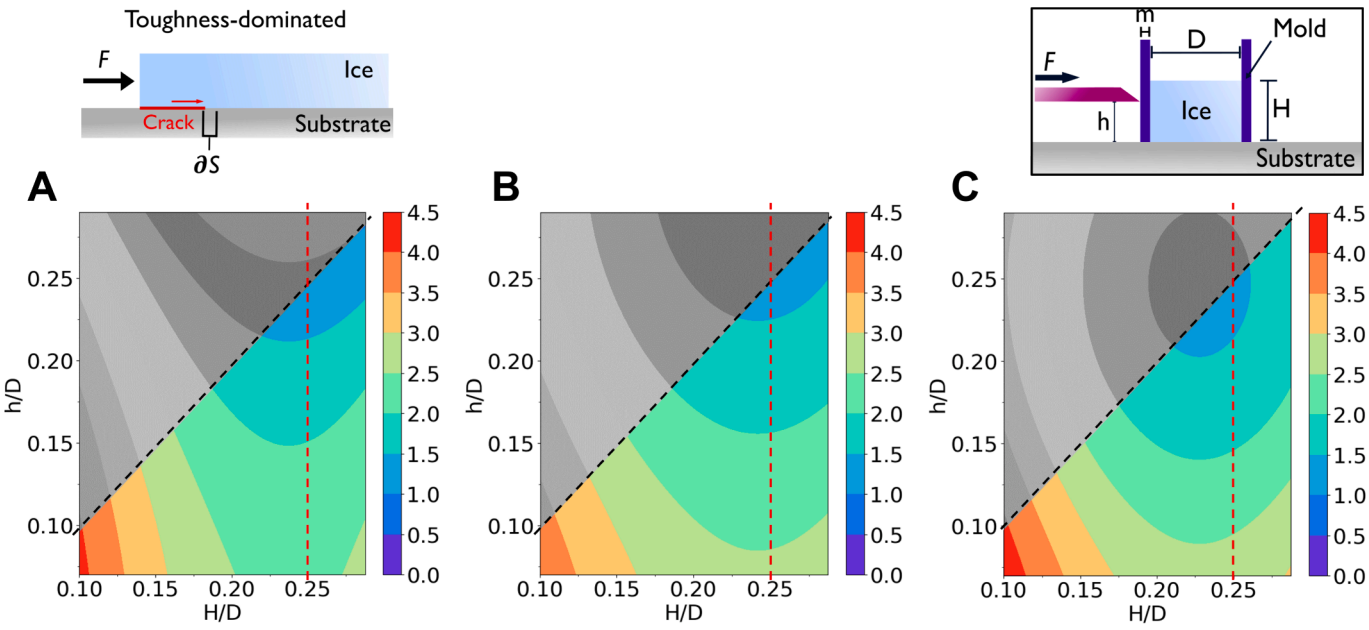

Fig. 3. Numerically calculated toughness parameters for (A) $\boldsymbol{m/D} = 0.2$, (B) $\boldsymbol{m/D} = 0.167$, and (C) $\boldsymbol{m/D} = 0.143$. The mold thickness $\boldsymbol{m}$ was kept constant at 2 mm and the ice diameter $\boldsymbol{D}$ was set to 10, 12, and 14 mm, respectively. The gray shaded area indicates the cases where the pushing height $\boldsymbol{h/D}$ is higher than the ice block thickness $\boldsymbol{H/D}$. At the same time, the experimental parameters should be chosen such that $\boldsymbol{H/D} < 0.25$. See SM Section S3 for plotting method. Inset: Representation of a horizontal push test with a cylindrical bulk ice sample.

Table 2
Interface toughness values for bulk ice on aluminum substrates.

Reference	Test Method	Toughness (G_{Ic}) [J/m^2]
Yeong et al. [30]	Pressurized air ice fracture test	0.72±0.11
Palanque et al. [14]	Electro-mechanical de-icing	0.38±0.09
Pervier and Hammond [31]	Pressurized air ice fracture test	0.95±0.45

the five experimental measurements are presented in Table 3. It can be noted that there is less variation in the force necessary to remove the ice column from the substrate compared to the stress-dominated case. Indeed, in a toughness-dominated case, the force does not scale with the interface area.

The numerical model is employed to retrieve the Toughness Parameter (TP) for each case, which is then utilized to calculate the interfacial toughness of the tested aluminum sample. The obtained interfacial toughness of the Al-6060 aluminum alloy was $G_{Tc} = 0.46 \pm 0.12 J/m^2$, based on our numerical model and experimental data. The value is in the range of the toughness values for aluminum reported in the literature (Table 2).

Table 3
Experimental data and computed $\boldsymbol{G_{Tc}}$. For each configuration characterized by *TP*, the force necessary to propagate the crack along the interface is measured and converted into an interfacial toughness value. The ratio of the standard deviation to the mean value ($\boldsymbol{\sigma(x)/\bar{x}}$) was calculated for the toughness ($\boldsymbol{G_{Tc}}$).

	Diameter [mm]	h/D	H/D	Applied Force [N]	*TP*	Toughness (G_{Tc}) [J/m^2]
	10	0.1	0.2	41.12	2.4	**0.45**
	10	0.1	0.25	53.98	2.1	**0.68**
	12	0.08	0.22	51.94	2.5	**0.43**
	14	0.07	0.19	59.74	2.8	**0.40**
	14	0.07	0.21	54.70	2.7	**0.32**
$\sigma(x)/\bar{x}$						**26.4 %**

3.3. Research approach

The stress and toughness analyses in this work are carried out on cylindrical ice samples. The contour plots presented in this work for the stress- and toughness dominated cases are therefore only valid for this specific ice sample geometry. As long as cylindrical ice samples are used, these plots can be used to characterize both the critical shear stress and the toughness of the substrates.

However, the analytical framework presented in this work is generally valid for push tests with any type of ice samples. If the shape of the ice sample is changed, e.g., a cubic ice block is used, the functions f and g presented in Eqs. (2) and (5) must be recalculated. The stress distributions, namely the SSIF, and the energy release rate for varying crack lengths must be analyzed as a function of the geometric parameters of the test system, such as h/D and H/D. The contour plots for the new ice sample geometry can then be constructed through FEM modeling.

Fig. 4 shows a generalized scheme for the stress and toughness analysis. In both cases, the experimentally determined force required to detach the ice is used together with the geometric parameters to calculate the desired quantity, τ_{min} and G_c, respectively. The functions f and g that relate the force F to τ_{min} and G_c are determined by FEM analysis.

4. Conclusions

We have shown how the average adhesion strength alone is not a sufficient measure of ice adhesion. For larger ice-substrate interfaces where crack propagation is controlled by toughness the adhesion strength becomes meaningless.

This work provides a novel conceptual framework for the horizontal push test to improve the accuracy of ice adhesion characterization. Firstly, in the stress-dominated fracture case, we propose SSIFs, which limit the dependency on geometric test parameters of the shear strength value. With the SSIFs, the true adhesion strength can be calculated, possibly reducing the discrepancies of shear strength values reported in literature.

Secondly, to provide a full characterization of the anti-icing material,

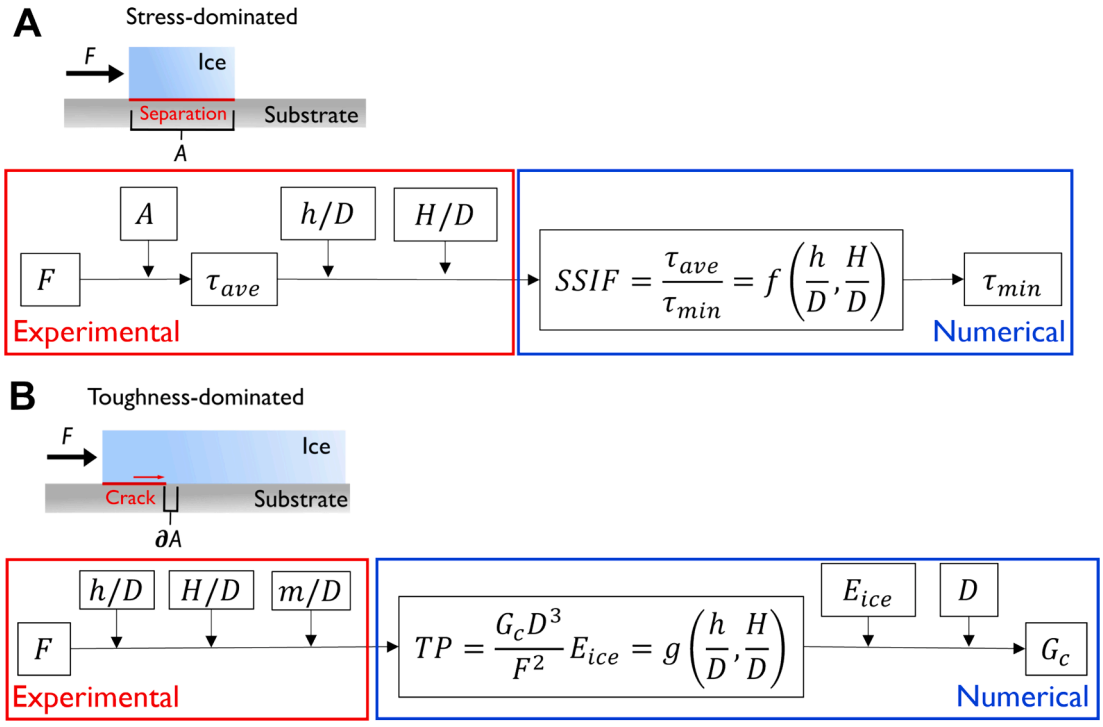

Fig. 4. Schematic representation of the mixed experimental and numerical research approach for (A) stress-dominated and (B) toughness-dominated detachment. The analysis can be extended to other geometries, and the proposed research approach remains valid, without losing generality.

this study proposes a methodology for toughness measurements with the horizontal push test. The total toughness can be calculated from the toughness parameters shown in Fig. 3 by knowing the test system parameters (h/D, H/D, and m/D) and the force necessary to propagate the crack.

The novel conceptual framework has been applied to a specific push test system and the results are still limited to a small set of experimental cases (i.e., cylindrical ice columns and fixed mold material), without differentiating between normal (G_I) and shear opening (G_{II}). It represents, however, a step towards standardization of icephobicity: only by understanding, recognizing, and assessing the different fracture mechanisms correctly, it is possible to reduce the discrepancies that can be found in the literature about ice adhesion measurements.

CRediT authorship contribution statement

Luca Stendardo: Writing – original draft, Visualization, Validation, Software, Methodology, Investigation, Formal analysis, Data curation, Conceptualization. **Giulia Gastaldo:** Writing – review & editing, Software, Methodology. **Marc Budinger:** Writing – review & editing, Supervision, Methodology, Formal analysis, Conceptualization. **Irene Tagliaro:** Writing – review & editing, Supervision, Project administration, Conceptualization. **Valérie Pommier-Budinger:** Writing – review & editing, Supervision, Methodology, Funding acquisition, Formal analysis, Conceptualization. **Carlo Antonini:** Writing – review & editing, Supervision, Project administration, Methodology, Funding acquisition, Conceptualization.

Declaration of competing interest

The authors declare that they have no known competing financial interests or personal relationships that could have appeared to influence the work reported in this paper.

Data availability

Data will be made available on request.

Acknowledgments

This project has received funding from the European Union's Horizon 2020 research and innovation programme under the Marie Skłodowska-Curie grant agreement No 956703 (SURFICE Smart surface design for efficient ice protection and control).

Appendix A. Supplementary material

Supplementary material to this article can be found online at https://doi.org/10.1016/j.apsusc.2024.160740.

References

[1] A. Work, Y. Lian, A critical review of the measurement of ice adhesion to solid substrates, Prog. Aerosp. Sci. 98 (2018) 1.
[2] A. Amirfazli and C. Antonini, Fundamentals of Anti-Icing Surfaces, in Non-Wettable Surfaces: Theory, Preparation, and Applications (The Royal Society of Chemistry, 2017).
[3] I. Tagliaro, A. Cerpelloni, V.-M. Nikiforidis, R. Pillai, C. Antonini, On the Development of Icephobic Surfaces: Bridging Experiments and Simulations, in: M. Marengo, J. De Coninck (Eds.), The Surface Wettability Effect on Phase Change, Springer International Publishing, Cham, 2022, pp. 235–272.
[4] S. Rønneberg, J. He, Z. Zhang, The need for standards in low ice adhesion surface research: a critical review, J. Adhes. Sci. Technol. 34 (2020) 319.
[5] D. Lou, D. Hammond, M.-L. Pervier, Investigation of the adhesive properties of the ice-aluminum interface, J. Aircr. 51 (2014) 1051.
[6] M. Schulz and M. Sinapius, *Evaluation of Different Ice Adhesion Tests for Mechanical Deicing Systems*, in (2015), pp. 2015-01–2135.
[7] L. Stendardo, G. Gastaldo, M. Budinger, V. Pommier-Budinger, I. Tagliaro, P. F. Ibáñez-Ibáñez, C. Antonini, Reframing ice adhesion mechanisms on a solid surface, Appl. Surf. Sci. 641 (2023) 158462.
[8] E. Martin, T. Vandellos, D. Leguillon, N. Carrère, Initiation of edge debonding: coupled criterion versus cohesive zone model, Int. J. Fract. 199 (2016) 157.
[9] K. Golovin, A. Dhyani, M.D. Thouless, A. Tuteja, Low-interfacial toughness materials for effective large-scale deicing, Science 364 (2019) 371.

[10] G. Gastaldo, V. Palanque, M. Budinger, V. Pommier-Budinger. *Stress and Energy Release Rate Influence on Ice Shedding with Resonant Electro-Mechanical De-Icing Systems*, in (Stockholm, Sweden, 2022).
[11] D. Leguillon, Strength or toughness? a criterion for crack onset at a notch, Eur. J. Mech. - ASolids 21 (2002) 61.
[12] M. Huré, P. Olivier, J. Garcia, Effect of cassie-baxter versus wenzel states on ice adhesion: a fracture toughness approach, Cold Reg. Sci. Technol. 194 (2022) 103440.
[13] M. Mohseni, L. Recla, J. Mora, P.G. Gallego, A. Agüero, K. Golovin, Quasicrystalline coatings exhibit durable low interfacial toughness with ice, ACS Appl. Mater. Interf. 13 (2021) 36517.
[14] V. Palanque, E. Villeneuve, M. Budinger, V. Pommier-Budinger, G. Momen, Cohesive strength and fracture toughness of atmospheric ice, Cold Reg. Sci. Technol. 204 (2022) 103679.
[15] V. Palanque, Design of Low Consumption Electro-Mechanical de-Icing Systems, Engineering Sciences [physics], Université de Toulouse; ISAE-Supaero, 2022.
[16] G. Gastaldo, M. Budinger, Y. Rafik, V. Pommier-Budinger, V. Palanque, A. Yaich, Full instantaneous de-icing using extensional modes: the role of architectured and multilayered materials in modes decoupling, Ultrasonics 138 (2024) 107264.
[17] Q. Yang, B. Cox, Cohesive models for damage evolution in laminated composites, Int. J. Fract. 133 (2005) 107.
[18] Z. Azimi Dijvejin, M.C. Jain, R. Kozak, M.H. Zarifi, K. Golovin, Smart low interfacial toughness coatings for on-demand de-icing without melting, Nat. Commun. 13 (2022) 5119.
[19] G. Hernández Rodríguez, M. Fratschko, L. Stendardo, C. Antonini, R. Resel, A. M. Coclite, *Icephobic gradient polymer coatings deposited via iCVD: a novel approach for icing control and mitigation*, ACS Appl. Mater. Interf. 16 (2024) 11901.
[20] T. Cebeci, F. Kafyeke, Aircraft icing, Annu. Rev. Fluid Mech. 35 (2003) 11.
[21] A. Klein-Paste, J. Wåhlin, Wet pavement anti-icing — a physical mechanism, Cold Reg. Sci. Technol. 96 (2013) 1.
[22] N. Rehfeld, et al., Round-robin study for ice adhesion tests, Aerospace 11 (2024) 106.
[23] L. Stendardo, G. Gastaldo, M. Budinger, C. Antonini, V. Pommier-Budinger, and A. C. Ospina Patiño, *Dynamic and Static Test Methods: Quantifying the Shear Strength at the Interface of Iced Substrates*, in (Vienna, Austria, 2023), pp. 2023-01–1451.
[24] F. Sanchez, M. Budinger, I. Hazyuk, Dimensional analysis and surrogate models for the thermal modeling of multiphysics systems, Appl. Therm. Eng. 110 (2017) 758.
[25] E.S. Taylor, Dimens. Anal. Eng. (1974).
[26] E. Buckingham, On physically similar systems; illustrations of the use of dimensional equations, Phys. Rev. 4 (1914) 345.
[27] J.R. Rice, A path independent integral and the approximate analysis of strain concentration by notches and cracks, J. Appl. Mech. 35 (1968) 379.
[28] *The J-Integral*, https://www.fracturemechanics.org/j-integral.html.
[29] A.T. Zehnder, Griffith theory of fracture, Encycl. Tribol. 1570 (2013).
[30] Y.H. Yeong, A. Milionis, E. Loth, J. Sokhey, A. Lambourne, Atmospheric ice adhesion on water-repellent coatings: wetting and surface topology effects, Langmuir 31 (2015) 13107.
[31] A.P. Ml, D.W. Hammond, Measurement of the fracture energy in mode I of atmospheric ice accreted on different materials using a blister test, Eng. Fract. Mech. 214 (2019) 223.
[32] A. Laroche, M. J. Grasso, A. Dolatabadi, and E. Bonaccurso, *Tensile and Shear Test Methods for Quantifying the Ice Adhesion Strength to a Surface*, in *Ice Adhesion*, edited by K. L. Mittal and C. -H. Choi, 1st ed. (Wiley, 2020), pp. 237–284.
[33] R.B. Sills, M.D. Thouless, The effect of cohesive-law parameters on mixed-mode fracture, Eng. Fract. Mech. 109 (2013) 353.
[34] I. Tagliaro, V. Radice, R. Nisticò, C. Antonini, Chitosan electrolyte hydrogel with low ice adhesion properties, Colloids and Surfaces A: Physicochemical and Engineering Aspects 700 (2024) 134695, https://doi.org/10.1016/j.colsurfa.2024.134695.